Optimizing Cobalt Ferrite Nanocrystal Synthesis Using a Magneto-optical Probe

Einat Tirosh, Gabriel Shemer, and Gil Markovich*

School of Chemistry, Raymond and Beverly Sackler Faculty of Exact Sciences, Tel-Aviv University, Tel-Aviv 69978, Israel

Received November 1, 2005

A modified approach toward synthesizing colloidal $CoFe_2O_4$ nanocrystals, using mixed types of organometallic precursors, is presented and compared to $CoFe_2O_4$ nanocrystals that have been produced according to previously reported synthetic techniques. Although the standard characterization techniques, such as electron microscopy, energy-dispersive X-ray spectroscopy, magnetometry, Fourier transform infrared spectroscopy, and X-ray diffraction, provided similar results for nanocrystals from three different syntheses, magneto-optical (MO) spectroscopy is the only technique that has revealed significant differences between these preparation techniques. The MO spectra displayed substantial differences in the incorporation of Co^{2+} ions within the ferrite crystal structure, making it a unique probe for optimizing the synthesis of stoichiometrically and structurally precise cobalt-ferrite nanoparticles.

Introduction

Technologically important bulk materials that contain a mixture of metal ions, such as metal oxides, are typically prepared by setting a precursor mixture with the temperature and pressure according to the equilibrium conditions of a desired phase.[1−5] Obtaining the correct phase of the same materials in the form of colloidal nanocrystal dispersion is more difficult, because the temperatures that can be applied in the synthesis of colloidal oxide nanoparticles are limited by solvent boiling/decomposition temperatures, which are usually much lower than the proper annealing temperatures required for achieving equilibrium structures in the bulk materials. At the elevated temperatures used in bulk materials synthesis, the colloidal particles would agglomerate and sinter to larger crystals. In addition, statistical concentration fluctuations in nanocrystal synthesis contribute to deviations from the desired stoichiometry with the possible accompanying deviations in crystal structure and electronic and magnetic properties.

Magnetic nanocrystals and, in particular, ferrite nanocrystals are of interest, because of their magnetic, magnetoresistive, and magneto-optical (MO) properties and their applications in ferrofluids,[6] magnetic storage devices,[7] site-specific drug delivery,[8] and magnetic resonance imaging.[9] Bulk ferrite materials are usually prepared by wet basic precipitation followed by annealing at high temperatures to obtain the desired crystalline structure.[10] Cobalt ferrite is a widely studied bi-metallic magnetic oxide, also in the form of colloidal nanocrystals, because of its relatively large magnetic anisotropy and large MO coefficients.[11] Many groups have synthesized colloidal cobalt ferrite nanoparticles, using various methods, such as water-in-oil microemulsions,[12,13] coprecipitation using microwave heating,[14] mechanical milling,[15] coprecipitation in an aqueous solution,[16] hydrothermal methods,[17] and a sol−gel-like technique.[18] Recently, novel high-temperature metal-organic salt decomposition techniques were used to obtain highly uniform size and shape controlled cobalt ferrite nanoparticles.[19−22] Most of these publications have provided magnetic measure-

* To whom correspondence should be addressed. E-mail: gilmar@post.tau.ac.il.

(1) Nasibulin, A. G.; Shurygina, L. I.; Kauppinen, E. I. *Colloid J.* **2005**, *67*, 1.
(2) Nieto-Sanz, D.; Loubeyre, P.; Crichton, W.; Mezouar, M. *Phys. Rev. B* **2004**, *70*, 214108.
(3) Andrault, D.; Bolfan-Casanova, N. *Phys. Chem. Miner.* **2001**, *28*, 211.
(4) Jung, I. H.; Decterov, S. A.; Pelton, A. D. *J. Phys. Chem. B* **2004**, *65*, 1683.
(5) Levy, D.; Diella, V.; Dapiaggi, M.; Sani, A.; Gemmi, M.; Pavese, A. *Phys. Chem. Miner.* **2004**, *31*, 122.
(6) Rosenweig, R. *Ferrohydrodynamics*; Cambridge University Press: Cambridge, U.K., 1932.
(7) Han, D. H.; Luo, H. L.; Yang, Z. *J. Magn. Magn. Mater.* **1996**, *161*, 376.
(8) Tae-Jong, Y.; Jun Sung, K.; Byung Geol, K.; Kyeong Nam, Y.; Myung-Haing, C.; Jin-Kyu, L. *Angew. Chem., Int. Ed.* **2005**, *44*, 1068.
(9) Cunningham, C. H.; Arai, T.; Yang, P. C.; McConnell, M. V.; Pauly, J. M.; Conolly, S. M. *Magn. Reson. Med.* **2005**, *53*, 999.
(10) Isfi, A. L.; Williams, C. M.; Johnson, A.; Nguyen, L. T.; Lodder, J. C.; Corcoran, H.; Chang; L.; Morgan, W. *J. Phys.: Condens. Matter* **2005**, *17*, 1399.
(11) Fontijn, W. F. J.; van der Zaag, P. J.; Feiner, L. F.; Metselaar, R.; Devillers, M. A. C. *J. Appl. Phys.* **1999**, *85*, 5100.
(12) Pillai, V.; Shah, D. O. *J. Magn. Magn. Mater.* **1996**, *163*, 243.
(13) Moumen, N.; Pileni, M. P. *Chem. Mater.* **1996**, *8*, 1128.
(14) Bensebaa, F.; Zavaliche, F.; Ecuyer, P. L.; Cochrane, R. W.; Veres, T. *J. Colloid Interface Sci.* **2004**, *277*, 104.
(15) Manova, E.; Kunev, B.; Paneva, D.; Mitov, I.; Petrov, L.; Estournes, C.; D'Orléans, C.; Rehspringer, J.-H.; Kurmoo, M. *Chem. Mater.* **2004**, *16*, 5689.
(16) Kim, Y. I.; Kim, D.; Lee, S. C. *Physica B* **2003**, *337*, 42.
(17) Cote, L. J.; Teja, A. S.; Wilkinson, A. P.; Zhang, Z. *Fluid Phase Equilib.* **2003**, *210*, 307.
(18) Meron, T.; Rosenberg, Y.; Lareah, Y.; Markovich, G. *J. Magn. Magn. Mater.* **2005**, *292*, 11.
(19) Sun, S. H.; Zeng, H.; Robinson, D. B.; Raoux, S.; Rice, P. M.; Wang, S. X.; Li, G. X. *J. Am. Chem. Soc.* **2004**, *126*, 273.
(20) Lee, Y.; Lee, J.; Bae, C. J.; Park, J. G.; Noh, H. J.; Park, J. H.; Hyeon, T. *Adv. Funct. Mater.* **2005**, *15*, 503.
(21) Liu, C.; Zou, B.; Rondinone, A. J.; Zhang, Z. J. *J. Am. Chem. Soc.* **2000**, *122*, 6263.
(22) Wang, X.; Zhuang, J.; Peng, Q.; Li, Y. *Nature* **2005**, *437*, 121.

10.1021/cm052401p CCC: $33.50
Published on Web 12/14/2005

ment data, showing large coercive fields at low temperatures for the synthesized nanoparticles, but did not present evidence for the relative distribution of Co^{2+} and Fe^{3+} ions between the two possible ferrite crystal sites of octahedral and tetrahedral oxygen coordination, nor did they study the statistical deviations from the ideal Co:Fe ratio of 1:2 between individual nanocrystals.

One of the main problems with the synthesis of mixed-metal-ion oxide particles such as $CoFe_2O_4$ is self-condensation of the two metal precursors to form segregated −Fe−O−Fe− and −Co−O−Co− regions. To obtain nanoparticles with high stoichiometric and structural uniformity in such materials, a selective chemistry to form preferentially −Co−O−Fe− bridges is desired. In this work, a new strategy using two different types of metal-organic precursors for the two metal ions has been developed toward achieving this goal. This mixed precursor method is similar to a strategy used by Brus and co-workers to produce $Hf_xZr_{1-x}O_2$ nanocrystals.[23] $CoFe_2O_4$ nanocrystals were synthesized using this method, which will be referred to as method A. The nanocrystal synthesis was performed at several temperatures to optimize the distribution of the Co ions in the ferrite lattice.

Cobalt ferrite corresponds to the group of spinel-type ferrites, which are compounds with a cubic oxygen lattice of the general formula $Me_xFe_{3-x}O_4$[24] where Me is usually a divalent metal cation. Fe_3O_4 (magnetite) is the prototype of an inverse spinel ferrite, with a cation distribution of $(Fe^{3+})[Fe^{3+}Fe^{2+}]O_4$. In this structural formula, the parentheses denote tetrahedral oxygen coordinated sites (A sites) and the square brackets denote the octahedral sites (B sites). The interstices of the coordination tetrahedra are too small for the larger Fe^{2+} ions, thus these sites are occupied by Fe^{3+} ions only. In $CoFe_2O_4$, it has been found that a certain percentage of Co^{2+} ions (up to 24% of the ions in the tetrahedral site), being smaller than Fe^{2+}, may replace the Fe^{3+} ions at the tetrahedral sites, while the majority of the Co^{2+} ions occupy the octahedral sites. It is thus impossible to refer to the cobalt ferrite lattice as having either the normal or the inverse spinel structure.[25] The rest of the Co ions replace the Fe^{2+} ions in the octahedral sites. These metal ion distributions can be observed spectroscopically, using MO spectroscopy, because extensive research has been performed on the MO properties of bulk ferrite films.[11,26−28]

In this work, MO spectroscopy was used as a primary electronic structure characterization tool, complemented by energy-dispersive X-ray spectroscopy (EDX) as a local stoichiometry probe, to compare the nanocrystals produced by method A at several temperatures to those produced by other, previously published synthesis procedures (methods B−D). The MO experiments revealed that the various synthesis products had different electronic structures, because of different distributions of the Co and Fe ions in the nanocrystal lattices, whereas magnetization and X-ray diffraction (XRD) studies were not able to detect these changes.

Experimental Section

$CoFe_2O_4$ nanoparticles were synthesized by several known synthetic methods. In addition, we have developed a modified synthetic method for obtaining cobalt ferrite nanoparticles (method A): 1.5 mmol of iron(III) acetylacetonate (Alfa Aesar), 0.5 mmol of iron(III) ethoxide (Alfa Aesar) (or alternatively iron(III) isopropoxide) and 1.0 mmol of cobalt(II) isopropoxide (Alfa Aesar) were added to 20 mL of benzyl ether (Aldrich) and stirred vigorously. The synthesis was performed at several different temperatures in the range of 230−300 °C by heating the solution to the desired temperature for 1−5 h under a nitrogen flow, in the presence of 6 mmol of oleic acid (Alfa Aesar) and 6 mmol of oleylamine (Aldrich). The resulting nanocrystals were precipitated by centrifugation at 6000 rpm for 5 min. The precipitate was dissolved in heptane and then a mixture of acetone and ethanol was added to the solution followed by centrifugation to obtain a size-selected precipitation of the nanoparticles. The other synthesis methods of cobalt ferrite nanoparticles were aqueous coprecipitation of Co^{2+} and Fe^{3+} ions[29] (method B), thermal-decomposition of the Fe and Co acetylacetonate precursors according to ref 19 (method C), and a sol−gel-like, high-temperature hydrolysis-based synthesis described in ref 18 (method D). The syntheses were performed exactly as described in the references. Cobalt oxide nanoparticles were prepared by adding 2 mmol of cobalt(II) acetylacetonate (Alfa Aesar) to 20 mL of benzyl ether with oleic acid and oleylamine and the solution was heated to 200 °C for 2 h.

Dilute solutions of the four synthesis products were drop-cast onto carbon-coated copper grids and inspected in a Tecnai F20 transmission electron microscope (TEM) system. EDX analysis of the individual particles was performed on 100 nanoparticles to obtain the atomic ratio between cobalt and iron in the various preparations. XRD patterns of a nanocrystalline precipitate were obtained with a Cu Kα radiation on a Scintag powder diffractometer.

SQUID magnetometry (Quantum Design, model MPMS XL5) was performed on nanoparticle samples that were deposited onto membranes. The nanoparticles were filtered through a membrane, the filtering paper was weighed with and without the nanoparticles and inserted into a capsule, and magnetization curves were measured at a temperature of 10 K.

A Fourier transform infrared (FTIR) (Vector, Bruker) spectrometer was used to measure the infrared absorption of the cobalt ferrite nanocrystals in the wavenumber range of 1000−400 cm^{-1} on pellets obtained by dispersing the samples in KBr.

Magnetic circular dichroism (MCD) spectroscopy in the visible part of the spectrum (1.45−3.35 eV) was performed on drop-cast nanocrystal films deposited on fused silica substrates. The MCD spectroscopy system consisted of a quartz-halogen lamp that was attached to an Oriel MS257 monochromator as a wavelength-selected light source and a Glan-Thompson polarizer attached at 45° to a Hinds photoelastic modulator as a polarization modulator. The monochromatic light, oscillating between right and left circular polarizations, passed through the poles of an electromagnet, through the sample located between these poles, and impinged on a photomultiplier. The detector output was separated into AC and DC components and the AC signal was lock-in amplified at the frequency of the modulator. The AC signal was divided by the DC

(23) Tang, J.; Fabbri, J.; Robinson, R. D.; Zhu, Y.; Herman, I. P.; Steigerwald, M. L.; Brus, L. E. *Chem. Mater.* **2004**, *16*, 1336.
(24) Antonov, V. N.; Harmon, B. N.; Antropov, V. P.; Perlov, A. Y.; Yresko, A. N. *Phys. Rev. B* **2001**, *64*, 134410.
(25) Sawatzky, G. A.; Van Der Woude, F.; Morrish, A. H. *Phys. Rev.* **1969**, *187*, 747.
(26) Fontijn, W. F. J.; van der Zaag, P. J. *J. Appl. Phys.* **1998**, *83*, 6765.
(27) Kim, K. J.; Lee, H. S.; Lee, M. H.; Lee, S. H. *J. Appl. Phys.* **2002**, *91*, 9974.
(28) Zang, H. Y.; Gu, B. X.; Zahi, H. R.; Lu, M.; Miao, Y. Z.; Zhang, S. Y.; Huang, H. B. *J. Appl. Phys.* **1994**, *75*, 7099.
(29) Fried, T.; Shemer, G.; Markovich, G. *Adv. Mater.* **2001**, *13*, 1158.

Table 1. Structural and Magnetic Properties of the Nanocrystals Taken from Transmission Electron Microscopy (TEM), Energy-Dispersive X-ray (EDX) Spectroscopy, and SQUID Magnetometer Measurements

	nanoparticle size [nm]	Co content [%]	lattice parameter [Å]	coercivity [kOe]	M_r/M_S
sample A	8.2 ± 1.5	21 ± 8	8.381 ± 0.002	15.6	0.83
sample B	10.8 ± 2.5	25 ± 6	8.339 ± 0.003	9.4	0.52
sample C	8.6 ± 1.2	22 ± 4	8.373 ± 0.003	16.5	0.77
sample D	11.9 ± 1.4	21 ± 4	8.378 ± 0.001	13.3	0.75

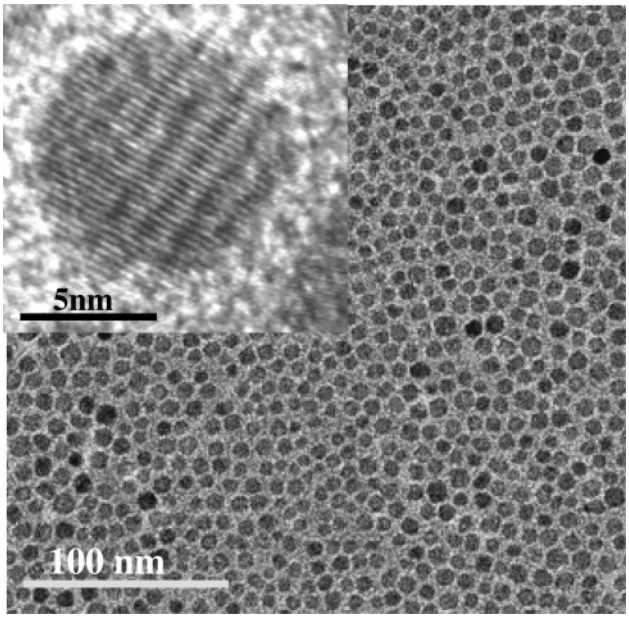

Figure 1. Transmission electron microscopy (TEM) image of $CoFe_2O_4$ nanoparticles prepared using method A at 270 °C. The inset shows a high-resolution image of a single nanocrystal.

signal to eliminate light intensity and detector sensitivity variations. The AC/DC signal is proportional to the magnetic circular dichroism ($\Delta\alpha$), which is the difference between the absorption of the right and left circularly polarized light ($\alpha_+ - \alpha_-$) at the sample subjected to a magnetic field parallel to the light propagation direction. Finally, to obtain the magnitude of the pure MCD coefficient, the AC/DC signal was divided by the absorbance (α) at each wavelength to normalize out differences in the optical extinction of the various samples ($\Delta\alpha/\alpha$).

Results and Discussion

The structural and magnetic measurement results for sample A synthesized at 270 °C are displayed in Table 1, together with those of the other samples. The TEM image of nanoparticles prepared by method A is shown in Figure 1. The inset shows a typical high-resolution TEM image, confirming that the nanoparticles prepared by method A are single crystals. The TEM images of samples B−D are displayed in Figure 2. EDX measurements over single particles provided the average atomic fraction of Co ions out of the total Fe + Co content within the nanoparticles (Table 1), which was lower than the cobalt precursor percentage inserted in the synthesis (33%), for all samples.

Representative XRD patterns for all of the samples are shown in Figure 3. They exhibit the typical pattern of a ferrite crystal structure. The lattice parameters are consistent with the bulk $CoFe_2O_4$ value (8.377 Å), except for sample B, where the lattice parameter was significantly shorter, comparable to maghemite (γ-Fe_2O_3, 8.346 Å). Because the lattice

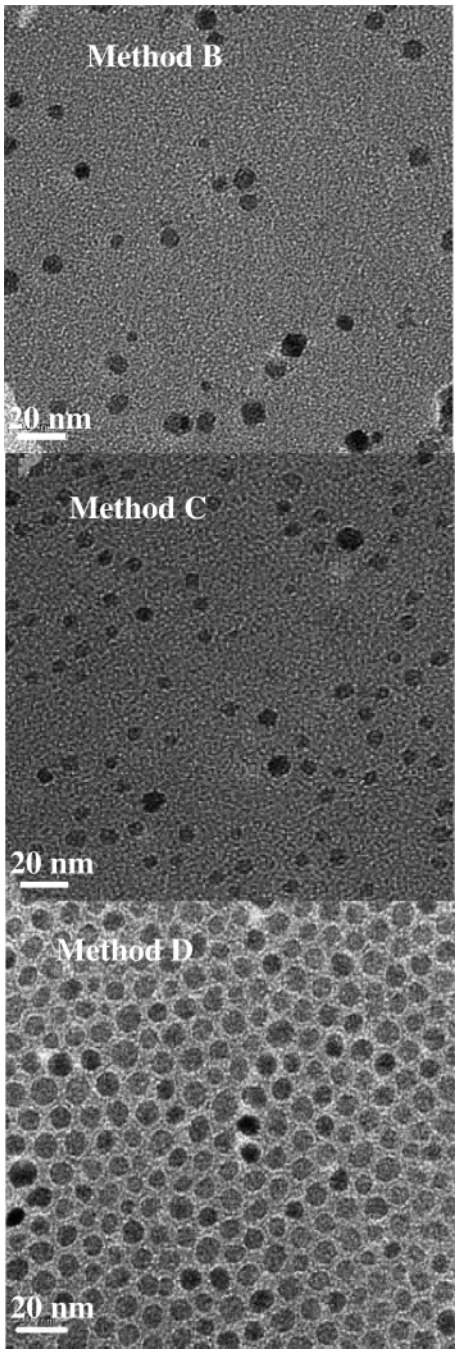

Figure 2. TEM images of $CoFe_2O_4$ nanocrystals prepared by methods B−D.

parameter of Fe_3O_4 (8.396 Å) is very similar to that of $CoFe_2O_4$, the XRD pattern should not be sensitive to the cobalt content of the nanocrystals or to the Co^{2+} distribution within the spinel lattice. A comparison of the obtained diffraction lines to those of cobalt oxide (Co_3O_4) did not yield a match in peak positions. Nanocrystal size estimates from Scherrer analysis of the diffraction line widths yielded

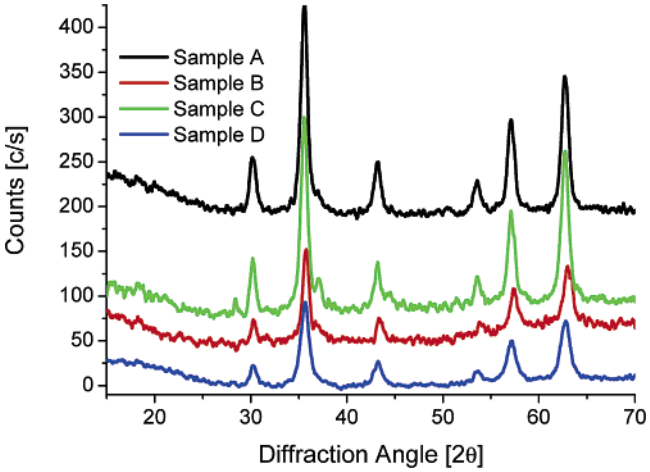

Figure 3. X-ray diffraction (XRD) spectra of $CoFe_2O_4$ nanocrystals prepared by methods A−D.

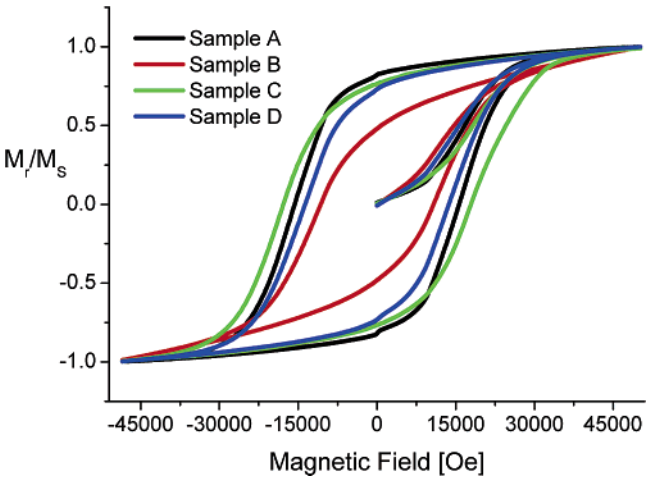

Figure 4. Magnetization curves for samples A, B, C, and D measured at a temperature of 10 K.

values that were very similar to those obtained from TEM statistics.

The 10 K hystersis curves for all the samples are shown in Figure 4. Except for sample B, the coercive fields of all samples were in the range of 13−16 kOe and the ratios of the remanent to saturation magnetizations (M_r/M_S) were similar to the expected value for isolated particles with cubic magnetic anisotropy (0.83). An M_r/M_S value, for sample B, of 0.5 is expected for uniaxial magnetic anisotropy, which is what one typically obtains for Fe_3O_4 and γ-Fe_2O_3 nanocrystals with relatively low magnetocrystalline anisotropy and dominant surface anisotropy. Thus, all the magnetic parameters of the nanocrystals produced by procedures A, C, and D were similar to those measured recently for procedure C[30] and for procedure D.[18] Saturation magnetization values were also similar to those measured for other synthesis schemes (on the order of 90 emu/g). The weighing error due to the surfactants attached to the nanocrystals did not allow extraction of an accurate M_S value.

Figure 5 displays the MCD spectra for all the samples. The bands in the MO spectra obtained for the synthesized nanoparticles matched the transitions reported by Fontijn et al. for bulk $CoFe_2O_4$ films using the MO Kerr effect.[11,26]

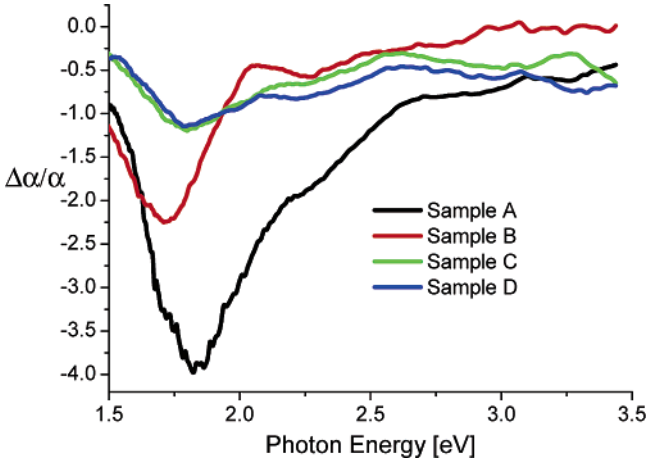

Figure 5. Magnetic circular dichroism (MCD) spectra of thin films of $CoFe_2O_4$ nanocrystals prepared by the four syntheses: (A) new method, (B) coprecipitation, (C) thermal decomposition, and (D) sol−gel-like synthesis.

For particles prepared by methods A, C, and D, a peak appeared at 1.80 eV corresponding to a crystal field (CF) transition of the Co^{2+}, $^4A_2 \rightarrow {}^4T_1(P)$, that is tetrahedrally coordinated. Sample B exhibited a peak shifted to 1.72 eV. A second peak appeared at 2.2−2.3 eV for all samples, corresponding to an intervalence charge transfer (IVCT), $[Co^{2+}]_{t2g} \rightarrow [Fe^{3+}]_{t2g}$ occurring at the octahedral interstices. For bulk samples, it has been found that the intensity of the CF transition is higher than that for the IVCT transition. In addition, the line width of the CF is significantly smaller than that for the IVCT transition.[11] Nanoparticles produced by method A exhibited the most intense signal for both of the peaks (~3 times larger than that observed for methods C and D). The intensity of the CF transition in the MCD spectrum is proportional to the occupation of the Co^{2+} ion at the tetrahedral site, whereas the second peak reflects the amount of Co^{2+} ions at the octahedral interstice. Thus, it is possible to conclude that only a small fraction of the Co^{2+} ions reside at both the tetrahedral and octahedral sites of samples C and D. Kalska et al. performed a detailed study of various ferrite nanoparticles synthesized by hydrolysis.[31] In their analysis of the MO Kerr spectrum, they have reached the conclusion that the cobalt ferrite nanoparticles, which exhibited very weak MO signature in the visible range have the Co^{2+} ions distributed between both types of sites. Thus, it seems that the synthetic method used by Kalska et al.,[31] as well as those of methods C and D, have not yielded a significant amount of Co^{2+} ions distributed at the crystal sites.

Figure 6 shows the MCD spectra of the $CoFe_2O_4$ nanocrystals prepared using method A at three different synthesis temperatures. As the temperature of the synthesis was increased, the intensity of the MO signal increased as well, indicating a significantly higher incorporation of Co^{2+} in the lattice at 270 °C, whereas the lower-temperature products resembled the results of syntheses C and D. Higher synthesis temperatures, up to 300 K, and longer synthesis durations did not change any of the measured physical properties relative to the synthesis at 270 °C for 1 h.

(30) Song, Q.; Zhang, Z. J. *J. Am. Chem. Soc.* **2004**, *126*, 6164.

(31) Kalska, B.; Paggel, J. J.; Fumagalli, P.; Rybzynski, J.; Satula, D.; Hilgendorff, M.; Giersig, M. *J. Appl. Phys.* **2004**, *95*, 1343.

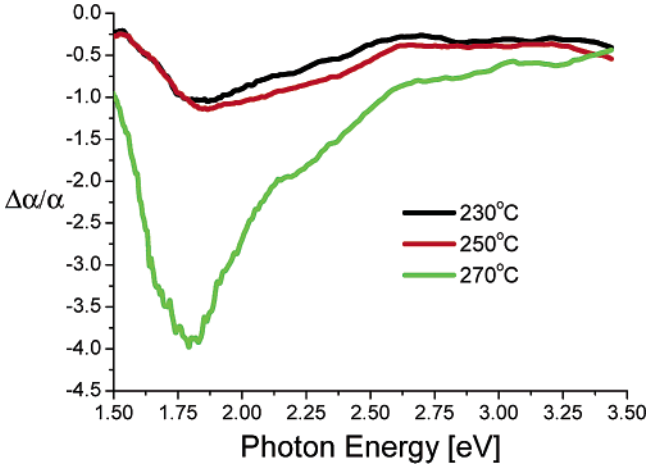

Figure 6. MCD spectra of thin films of $CoFe_2O_4$ nanocrystals prepared via method A at various temperatures.

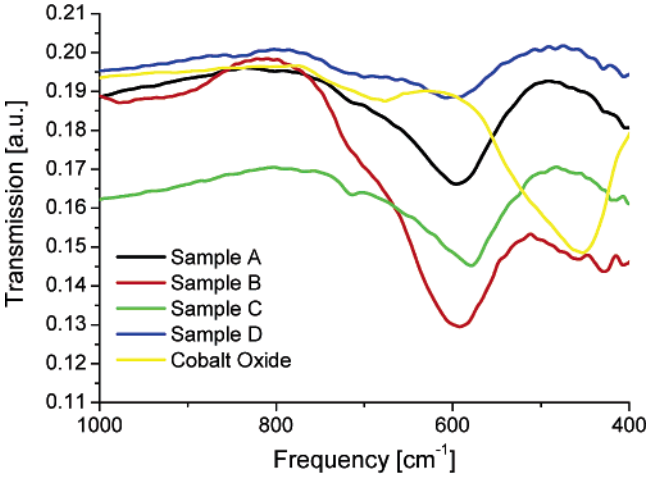

Figure 7. Fourier transform infrared (FTIR) spectra of nanoparticles produced via methods A−D, in comparison to cobalt oxide nanoparticles.

The FTIR absorption spectra of the samples shown in Figure 7 exhibited an intense peak at ∼590 cm^{-1} that is characteristic of the Fe−O stretching phonon of cobalt ferrite[32] and a weak shoulder at ∼710 cm^{-1} that is probably associated with Co_3O_4[33] and seems to be smaller at sample A. Both sample B and the cobalt oxide sample showed a peak at 450 cm^{-1}, indicating the presence of Co_2O_3 (or CoOOH) and CoO.[34]

Sample B, which was prepared using a coprecipitation hydrolytic method, showed significant differences in its physical properties, in comparison to all other samples. Its coercivity and M_r/M_S values were significantly lower, the MO peak was shifted, in correlation with the shorter lattice constant, relative to the other samples, and its FTIR spectrum showed an additional peak, which did not appear in the spectra of the other samples. It can thus be concluded that the preparation of cobalt ferrite nanocrystals using method B resulted in a more-defective lattice, more similar in structure to γ-Fe_2O_3, with a higher degree of cobalt oxide phase segregation. In addition, the apparent uniaxial magnetic anisotropy of these nanocrystals probably indicates strong inhomogeneities in the nanocrystals.

The results of the MO spectroscopy experiments show that only when specific synthesis conditions were used, a major amount of Co^{2+} ions was incorporated in the ferrite lattice. There are two possibilities regarding the location of the Co ions, which were observed by the EDX measurements but were missing from the ferrite lattice sites in samples C and D. The first and more-likely possibility is the formation of a segregated oxide phase, either crystalline or amorphous, probably at the nanocrystals surfaces, and the second is the oxidation of the Co^{2+} to Co^{3+} at the ferrite interstices, accompanied by a corresponding Fe^{3+} reduction to Fe^{2+} to maintain charge neutrality, which is electrochemically less favorable.

The FTIR spectra of samples A, C, and D exhibited distinct characteristics of the $CoFe_2O_4$ structure with a small amount of Co_3O_4, indicating that some of the missing Co ions have oxidized into the trivalent state. In synthesis D, which is a hydrolytic process performed under oxidizing conditions, the oxidation of some of the Co^{2+} ions to Co^{3+} ions to form Co_3O_4 is very likely. However, synthesis C was performed in the presence of a mild reducing agent (hexadecanediol), which is absent from process A. Thus, in this case, the significant differences in Co^{2+} inclusion between syntheses A and C cannot be simply explained by differences in the oxidation state of cobalt. The magnetic measurements revealed only small differences between the samples (apart from sample B), whereas the MO spectra revealed significant changes. The relative insensitivity of the coercivity on Co^{2+} content can be explained by the small amount of Co ions required to obtain the large magnetocrystalline anisotropy observed in cobalt ferrite. Experiments on $Co_xFe_{3-x}O_4$ with varying x have shown that the magnetic anisotropy contributed by one Co ion to magnetite is more than 100 times larger than that of one Fe ion.[35] Saturation magnetization should also be insensitive to the Co^{2+} replacement of Fe^{2+}, as evidenced from the small differences in saturation magnetization between $CoFe_2O_4$ (90 emu/g) and Fe_3O_4 (80 emu/g).

Consequently, in contrast to other synthesis schemes, the new, hybrid precursor, thermally assisted non-hydrolytic condensation synthesis seems to produce nanocrystals that are similar in ionic configuration to bulk cobalt ferrite, having a crystal structure where the Co^{2+} ions occupy both octahedral and tetrahedral sites. The technique involves a reaction between cobalt isopropoxide and iron acetylacetonate, which forms the Fe−O−Co bridges needed to obtain the cobalt ferrite. This process is analogous to nonhydrolytic sol−gel preparation schemes, in which a condensation between two different precursors, such as metal halide (or metal carboxylate) + metal alkoxide occurs through alkyl halide (or ester) elimination.[23,36,37] Such mixed precursor chemistry has the potential to form preferentially the mixed-metal oxide networks (−Fe−O−Co−O−Fe−) under con-

(32) Huang, X.; Chen, Z. *J. Cryst. Growth* **2004**, *271*, 287.
(33) Ahmed, S. R.; Kofinas, P. *J. Magn. Magn. Mater.* **2005**, *288*, 219.
(34) Tarasevich, M. R.; Efremov, B. N. In *Electrodes of Conductive Metallic Oxides, Part A*; Trasatti, S., Ed.; Elsevier: New York, 1980; p 221.
(35) Slonczewski, J. C. *Phys. Rev.* **1958**, *110*, 134.
(36) Vioux, A. *Chem. Mater.* **1997**, *9*, 2292.
(37) Pinna, N.; Garnweitner, G.; Antonietti, M.; Niederberger, M. *Adv. Mater.* **2004**, *16*, 23.

trolled temperature conditions and suppress self-condensation of the iron or cobalt precursors to form segregated oxide phases within the nanocrystals.

The achievement of control over cation distribution in the ferrite particles is apparently less important in the case of tuning the magnetic properties of the nanocrystals and is more important in the case of using the nanocrystals for MO applications. Moreover, this study is a significant milestone in the development of general preparation schemes of stoichiometrically controlled multication oxide nanocrystals and in the application of suitable characterization probes.

Conclusion

A modified technique for synthesizing cobalt ferrite nanoparticles, which is based on mixed types of metal-ion precursors, has been presented. The concept of using mixed types of organometallic precursors to prepare complex oxide nanocrystals may offer a route to optimize their structure and properties. The favorable method for monitoring the distribution of magnetic ions within ferrite nanocrystals seems to be magneto-optical (MO) spectroscopy, where it is possible to correlate between the electronic transition's intensity and the concentration of the metal ions directly in the corresponding crystal site. Further control of the occupation of lattice sites by Co^{2+} could be achieved by doping the nanocrystals with other metal ions.

Acknowledgment. This work was supported by the Israel Science Foundation (Grant No. 208/03) and the James Frank Program. We are grateful to Dr. Yuri Rosenberg for the XRD measurements.

CM052401P